ОБЪЕДИНЕННЫЙ
ИНСТИТУТ
ЯДЕРНЫХ
ИССЛЕДОВАНИЙ

Дубна

E13-2001-204

E.S.Kuzmin, A.M.Balagurov, G.D.Bokuchava, V.V.Zhuk,
V.A.Kudryashev*, A.P.Bulkin*, V.A.Trounov*

DETECTOR FOR THE FSD FOURIER-DIFFRACTOMETER BASED ON ZnS(Ag)/ ^{6}LiF SCINTILLATION SCREEN AND WAVELENGTH SHIFTING FIBERS READOUT

Submitted to the «Journal of Neutron Research»

33/17

*St. Petersburg Nuclear Physics Institute, Gatchina, Russia

2001

1. INTRODUCTION

The luminosity of a neutron spectrometer increases linearly with the solid angle and efficiency of the detector array. Recently, a way to increase the solid angle to a considerable extent preserving high instrumental *d*-spacing resolution has been proposed for time-of-flight Fourier diffractometer for stress measurements [1]. The method consists of combined application of electronic and geometrical time-focusing techniques for multielement detector. However, to realize this method, one has to develop large aperture thermal neutron detector possessing a number of particular properties.

The geometrical component of TOF diffractometer resolution function may be reduced to the level of time component (about 10^{-3}) if the sensitive layer of each detector element is well tailored to the particular Time-Focusing Surface (TFS), and the thickness of sensitive layer does not exceed several millimeters. In addition, common requirements to thermal neutron detectors, such as high neutron efficiency (better than 50%) and low gamma sensitivity (about 10^{-7}), have to be met.

Some of these requirements (thickness limitation and tailoring to specific surface) exclude definitely the usage of gaseous counters for this purpose. The experience of lithium glass application [2] demonstrates that gamma sensitivity reduction is very desirable and the tailoring of glass scintillator to TFS is rather difficult and complicated. Therefore, to realize the idea of combined focusing for a new high-resolution diffractometer (FSD) [3], the scintillation screen, available on the market under trade name ND [4], has been selected.

The screen is composed of two polycrystalline powders - ^{6}LiF as a neutron capturer and ZnS(Ag) as a scintillator - bound with acrylic resin. The screen has a degree of flexibility making it possible to achieve the better tailoring to TFS in comparison with plain glass scintillators due to usage of curved surfaces. The distinctive features of zinc sulfide scintillator are its well-known extremely low gamma sensitivity due to a high value of α/β - ratio (ratio between the response to fast electrons and alpha-particles) and high scintillation efficiency, comparable to that of NaJ(Tl).

However, a number of drawbacks limit its application for neutron detection. The presence of several slow components with decay time exceeding tens of microseconds in the light emission of zinc sulfide powder makes it necessary to use special methods of signal processing. Due to high refraction index of ZnS(Ag) crystal (n=2.4) the screen represents a high disperse medium with a diffuse light transmission. Screen surfaces have a high roughness on account of the technology of its manufacturing. Therefore, the widespread methods of light collection, based on a high transparence of a scintillator and the effect of total internal reflection cannot be used even at small size detector development.

For the proposed detector geometry with close-packed element arrangement, it is unacceptable to locate photomultipliers in arbitrary manner. Moreover, complete overlapping of the sensitive area by photo cathodes is very expensive design approach for large aperture counters. Therefore, the examination of the method of Wavelength Shifting fibers (WLS) readout from large area ND screen is undoubtedly of interest.

The goal of the research performed was the development of time-focused thermal neutron large aperture detector on the base of scintillation screen ND and WLS fibers readout for FSD instrument. In this article, the design and performance of the detector developed are presented. In section 2, the studied properties of light emission from ND screen are reported. Signal discrimination technique and associated electronics are described in section 3. In section 4, the method of TFS approximation is offered. Detector design is described in section 5 and beam test result is reported and discussed in section 6.

2. PROPERTIES OF LIGHT EMISSION FROM ND SCREEN

In the composition of ND screen the zinc sulfide activated with Ag is used in a powder form with the average size of a grain D=4.5 micron. Light emission performances of powder scintillators depend significantly on a grinding method and size distribution of grains, therefore the waveshape of light pulses was measured individually under irradiation of supplied samples of screen with thermal neutrons. For this purpose the counter was fabricated on the base of Photonis XP2262 photomultiplier [9], where small (20x20 mm^2) sample of the screen was suspended in a reflecting optical trap apart 16 mm from PM input window.

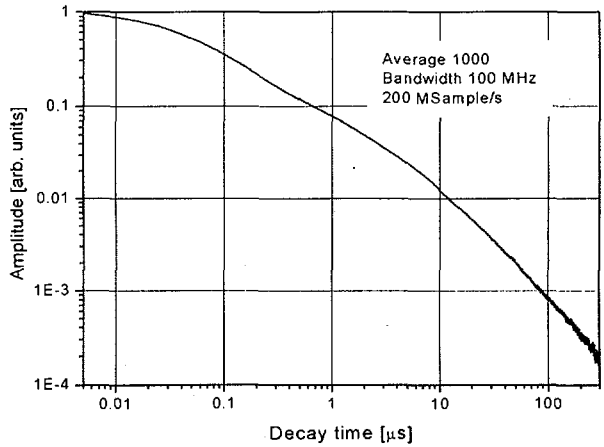

Figure 1. Decay curve of ND screen irradiated by thermal neutrons.

For waveshape measurement, the anode current pulse was analyzed with digital oscilloscope (Tektronix TDS340A), operating at a sample frequency of 250 MS/s. The time spectra, of up to 1000 channels were transferred on-line through GPIB interface to a personal computer. Spectra were stored and processed with the help of LabView code.

The average waveshape for 1000 pulses was measured with consecutive shifting of digital window with respect to pulse leading edge. Average waveshape under thermal neutron irradiation of the screen is given in Figure 1.

In the time range examined, the trailing edge of the waveshape is analytically well described by the sum of seven exponential terms:

$$A = \sum_{i=1}^{7} A_i \cdot \exp(-t/\tau_i);$$

ZnS(Ag) exhibits decay time constants from tens on nanoseconds to one hundred of microseconds, but the most powerful components (1 – 4) have decay time less than 1 μs. The results of fitting are shown in Table 1.

Table 1. Decay curve fitting results.

Component	1	2	3	4	5	6	7
Decay Time τ_i (μs)	0.022	0.074	0.208	0.881	4.3	18.1	87.7
Coefficient A_i	191.1	229.5	88.3	497.	25.1	5.9	1.2

Typical oscillograms of individual event of light emission are shown in Figure 2. It may be seen, that the process of the light emission from zinc sulfide is realized as a series of separate pulses generated by flash outs of individual luminescence centers of the scintillator. The width of pulses is determined by the time constant of the photomultiplier anode circuit (load resistance 50 Ohm).

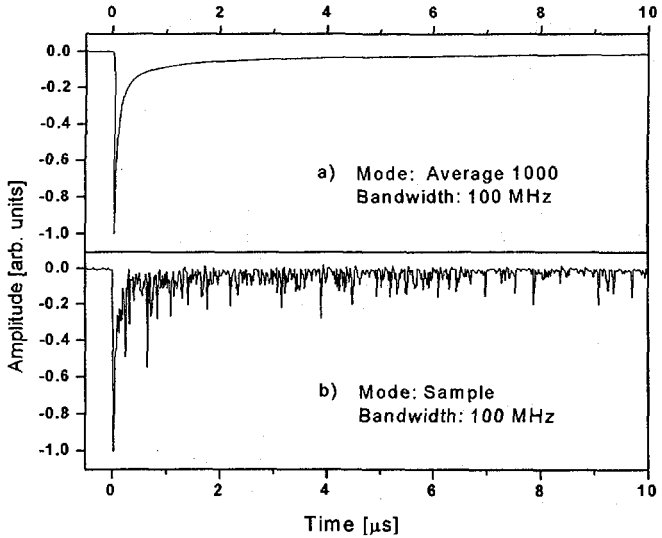

Figure 2. Shape of the light pulse produced in ND screen by neutron capture event: (a) averaged (1000 events) waveshape; (b) individual pulse.

The distinctive feature of ZnS(Ag) crystal is an increased (in comparison with other scintillators) average power of individual luminescence center and a relatively small number of them.

At the beginning of light emission process, the flash out frequency of individual centers is high, and it is possible to single out a rather wide resultant pulse with fall time, determined by fast components. Total decay time of light emission process is not determined by slow components, which have been found, but it is considerably longer due to afterglow of the scintillator.

A significant disadvantage of the screen is extremely wide dynamic range of optical pulses, generated after neutron capturing, up to 60 dB. The major cause of dynamic range expansion is a poor transparency of the screen to its own luminescence originated by already mentioned high value of the refractive index of ZnS(Ag) crystal. Light losses are so high, that even with double-side light collection it is possible to effectively utilize the screen with thickness up to some tenths of millimeter only.

3. PULSE DISCRIMINATION METHOD

For the effective exploitation of a large aperture detector in neutron TOF Fourier diffractometry, its minimum pulse resolution should not exceed a few microseconds under the neutron flux on a sample at a level of 10^6 n/s. From the data shown in Table 1, the nature of waveshapes in Figure 2, and also taking into account a large pulse range it appears that with the help of pulse discrimination on a constant threshold it is extremely difficult to separate fast component signal from slow component flash outs under the restriction imposed on minimum pulse resolution of the detector. Therefore, we have used a method of double signal discrimination, similar to that described in [5]. In our case, the method is used to discriminate the desired signal generated by fast components against the unwanted background of slow components. The discrimination set-up based on standard electronics is shown in Figure 3.

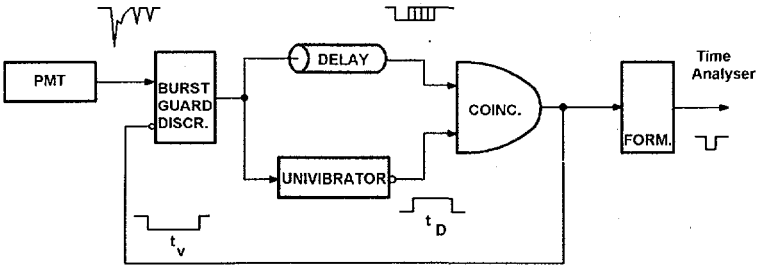

Figure 3. Schematic representation of the discrimination set-up.

The anode signal of a Photonis XP2262 photomultiplier tube is sent to a LeCroy 821 discriminator operating in "burst guard" mode. In this mode, the output signal duration is equal to the time-over-threshold of the input signal. Further selection of signals of constant amplitude is carried out by pulse duration discriminator, which consists of two LeCroy 622 Logic units. Pulse duration threshold (t_D) is determined by the preset width of the complementary output of 622 unit used as a monovibrator. The second unit 622,

exploited as a coincidence, enables to reject pulses, delivered by discriminator 821, which duration is less than a preset threshold.

At the initial stage of light emission process, (of the order of a few microseconds) the frequency of short pulses generated by slow components is very high, up to 100 MHz. At this frequency, a false operation of the duration discriminator is possible and as a result, a neutron may be registered twice. It has been found that events of two types may cause a malfunction of the duration discriminator. In the first case, some pulses, delivered to coincidence unit by discriminator 821 at the presence of complementary signal from monovibrator, continue to act after the termination of that signal. To eliminate a false counting in such cases the monovibrator must be retriggered before the end of an output pulse and therefore an updating unit (622) was used.

Another opportunity of malfunction arises, when in addition to the main pulse with $t > t_D$ generated by fast components, the second one is formed at the random superimposition of short pulses from slow components, with the duration exceeding a threshold of discrimination.

To provide the rejection of such events, signal processing is vetoed for a time t_V, determined by output pulse duration of coincidence unit. The negative output of coincidence unit feeds back amplitude discriminator via its respective veto input to make it nontriggerable within t_V. As the final shaper of output signal, delivered to time analyzer, LeCroy 623B discriminator was used.

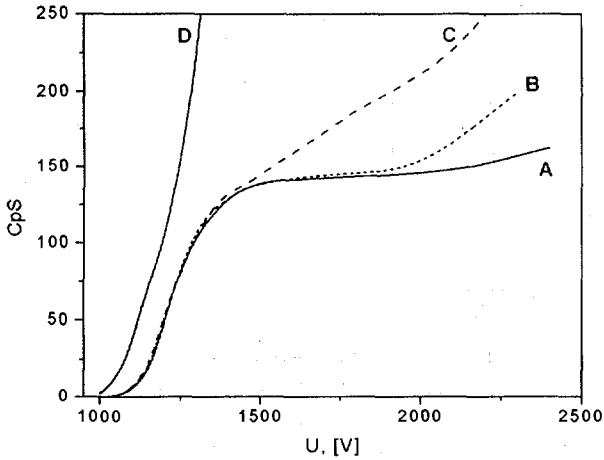

Figure 4. Counting response curves of small area detector with air lightguide. Curves A – C were registered for amplitude discrimination level – 30 mV and pulse duration threshold – 100 ns. Curve A – veto signal duration $t_V = 2$ μs; curve B - $t_V = 0.6$ μs; curve C – veto signal disconnected. Curve D was registered without pulse duration discriminator.

It appears that the optimum value of time threshold is in the limits from 100 to 300 ns and it depends on the light collection efficiency of the detector and the bandwidth of analog signal. The dead time of the discrimination setup is equal to the sum of veto

signal duration and the preset time threshold ($t_M = t_V + t_D$). Time resolution of the detector is determined by the duration of fast component leading edge, which does not exceed 10 ns. Discrimination setup efficiency is demonstrated in Figure 4, where counting response curves for the small area detector with air lightguide are shown. The presence of plateau with a length depending on veto signal duration is the evidence of counting stability.

For detectors with WLS-fiber lightguide the light collection efficiency does not exceed 4% and photoelectron statistics in a pulse formed by fast components deteriorates to such an extend that some pulses get broken in parts and cannot pass the duration selection procedure. To avoid registration efficiency losses for such detectors, the anode signal band was artificially limited to a level of 6 MHz. The type of low-pass filter and signal bandwidth were fitted experimentally.

The described method of discrimination allows effective rejection of unwonted signals of various origins, such as photomultiplier noise; slow components induced pulses and the signals, generated in WLS-fibers material by gamma rays. In Table 2, the values of rejection factor for two types of counters are given – for the small ones (sensitive surface S = 4 cm^2) with light collection via air lightguide and for the full-scale counter (S = 540 cm^2) of WLS-fibers readout.

Table 2. Suppression ratio for unwanted signals of various origins.

Signal origin	Suppression Ratio	
	Air Lightguide *	WLS Fibers **
Photomultiplier noise	$\leq 1 \cdot 10^{-6}$	$4 \cdot 10^{-5}$
Gamma-background	$\leq 1 \cdot 10^{-8}$	$7 \cdot 10^{-7}$
Slow components flash outs	$2.7 \cdot 10^{-6}$	$4.5 \cdot 10^{-5}$

* - Bandwidth 100MHz.
** - Bandwidth 6 MHz.

4. DETECTOR GEOMETRY

The detector system of Fourier stress diffractometer should have the largest feasible solid angle of observation to obtain data of high statistical accuracy for small gauge volume with acceptable experiment duration. Simultaneously, the geometrical component of the diffractometer resolution function should not exceed time component noticeably. The method of geometrical time focusing [6] used so far in neutron TOF diffractometry has one essential limitation. Linear dimensions of a geometrically focused detector expand drastically with an increase of the solid angle. Therefore, the principle of the combined electron-geometry focusing was proposed in [1]. In this method, the region of interest of the scattering angle has to be divided into a few parts with individual TFS, and a separate counter has to be developed for each bearing sector. Figure 5 shows the arrangement of sensitive layers in the detector bank of 90-degree detector of combined electron-geometry focusing.

In an ideal case the sensitive layer of each module should coincide with TFS, which is the surface of revolution of Time Focusing Curve (TFC) around the axis of incident neutron beam.

TFC may be represented by the equation in polar coordinates (R, θ), where polar axis coincide with the axis of neutron beam and has the origin in the sample center:

$$[A_0 + R(\theta/2)]\cdot\sin(\vartheta/2) = [A_0 + R_0(\vartheta_0/2)]\cdot\sin(\vartheta_0/2);$$

where A_0 is a distance between Fourier chopper and the center of the sample, (R_0, θ_0) are coordinates of the initial point of TFC.

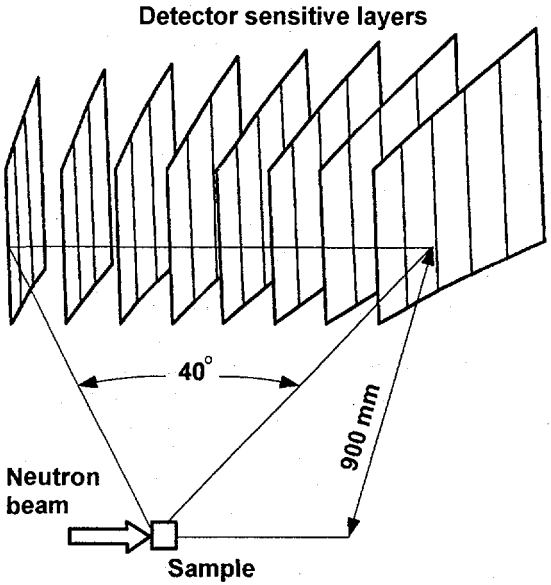

Figure 5. The layout of the detector bank focused under the combined electron-geometry method.

Practically one has to select the method of TFC approximation depending on the scintillator used. To fabricate detectors of the previous generation [3] with lithium glasses the sensitive surface was fitted from the disks of 1 mm thickness. The screen used in our case possesses some flexibility making it possible to use curved surfaces for TFS approximation. The design approach of such kind is surely more complicated but it enables to exclude completely the dead zone of solid angle of observation and drastically reduce the average error of TFS approximation.

To develop the first modules of 90-degree detector, three conical surfaces have been used for TFS approximation, and therefore, the detector was named MultiCon. At the first stage, the piecewise approximation of TFC has been derived and then polygon legs were revolved around neutron beam axis to cover the azimuth-viewing angle of the detector. The scintillator screen should exactly reproduce tapered surfaces patterns obtained in this way.

Detector's geometry calculation in accordance with the method, developed in [7] was carried out. The relative error of the flight path η was determined by a set of all eventual paths of neutron passing through the gauge volume and sensitive layer:

$$\eta = [L_r(\theta) - L(\theta)] / L(\theta),$$

where $L(\theta)$ is the distance from Fourier chopper to the time focusing surface at scattering angle θ, and $L_r(\theta)$ is the real flight path to the approximating surface. The aim of the optimization was to find the amount of tapered surfaces and their arrangement for the given solid angle of acceptance of the complete detector. The optimization has been carried out under following conditions: the mean value of flight path relative error $m(\eta)$ must be equal to zero, $m(\eta)=0$, and its standard deviation was limited with a given value $\sigma(\eta)<\sigma_{max}$, where σ_{max} is derived from the given instrumental resolution.

5. DETECTOR DESIGN

FSD 90-degree MultiCon detector consists of two banks, each centered on a scattering angle (2θ) of $\pm 90°$. These detector banks are composed of eight modules stacked horizontally (Figure 5) covering an angular range from $\pm 70°$ to $\pm 110°$ in 20. Each separate module covers the solid angle $\Delta\Omega = 0.020$ sr. The proposed detector geometry possesses a number of advantages but makes it practically impossible to apply the conventional method of light collection by coupling photomultipliers directly to scintillator. The distance between the adjacent TFS is too small for the photomultiplier arrangement. Therefore, it has been proposed to exploit the method of light collection with the help of Wavelength Shifting (WLS) fibers. All sensitive area of the counter is covered with fibers, and blue scintillation light, emitted from the screen, is absorbed in fiber core material and then reemitted with wavelength spectrum shifted towards green region. Since secondary photons are emitted from within the fiber, they may be transmitted by the effect of total internal reflection to the entrance window of a photomultiplier.

Two identical modules of 90-degree detector on the base of ND screen and WLS fibers readout have been fabricated and tested on the FSD beam. The sensitive layer of these modules with total area of 540 cm^2 is composed of three sections of different conical surfaces. ND-screen patterns were glued to honeycomb structure support with a geometry precision better that 0.3 mm.

WLS-fibers of 1 mm in diameter (BCF-91A [8]) and with a decay constant τ=12 ns were located on both sides of scintillation screen. On the back surface, the fibers were fixed with a pitch of 2.5 mm at a distance of 4 mm from the screen. On the front side the distance from the screen surface was increased up to 100 mm in order to avoid the disturbance of neutron flux. Beyond the bounds of sensitive layer, the fibers were gathered in two bundles and connected via air lightguide to the entrance window of XP2262 photomultipliers.

6. BEAM-TEST RESULTS OF MULTICON DETECTOR

For comparative test purposes the first module of the detector under development and lithium glass detector of previous generation (DPR) were installed together on the neutron beam of Fourier stress diffractometer. The data were taken simultaneously from both detectors. Detector DPR has been shielded with 50 mm layer of lead against gamma rays and with another layer of borated polyethylene to reject neutron background. The module developed on the base of ND screen was wrapped in a sheet of cadmium only.

Table 3. Operating characteristics of the detectors developed on the base of lithium glass and ND-type screen.

Detector	DPR	MultiCon
Average Scattering angle, 2θ	90°	107.5°
Sensitive Layer Material	Li – Glass	ZnS (Ag)/^{6}LiF (ND)
Sensitive Layer Thickness	1 mm	0.43 mm
Light Collection Method	Direct Coupling	WLS-Fibers
Counters Number	16	8
Single Counter Solid Angle	$(1.5 - 3.6)\cdot10^{-3}$ sr	0.018 sr
Total Solid Angle	0.036 sr	0.144 sr
Nuclear Efficiency *	94 %	62 %
Electronic Efficiency	100 %	92 %
Total Efficiency	94 %	57 %
Effect/Background Ratio	1.9	3.7
Minimum pulse separation	200 ns	2 μs
Intrinsic noise	Not measured	≤ 1 cps
Gamma - Sensitivity	Not measured	$\leq 7\cdot10^{-7}$
Total resolution $\Delta d/d$ (d=2 Å) -Time component -Geometric component	$5.5\cdot10^{-3}$ $1.2\cdot10^{-3}$ $5.3\cdot10^{-3}$	$3.8\cdot10^{-3}$ $1.6\cdot10^{-3}$ $3.4\cdot10^{-3}$

* - Average slide angle ~20°

Test results are presented in Table 3. It can be seen from the data presented in Table 3, that the nuclear efficiency of lithium glass based detector is half as much again than for MultiCon module. This result may be explained taking into account that lithium glass is two times thicker than ND screen while lithium atom concentration is equal for both scintillators. Insignificant loss of MultiCon electronic efficiency is caused by the fact that the method of TFS approximation does not match well with WLS fiber readout. The minimal bending radius (about 20 cm) of the fibers does not allow arranging them at an equal distance from the screen along overall sensitive surface. Therefore, no high

uniformity of light collection can be provided and a few percent of neutron capture events generating small amount of photoelectrons on the photocathode are rejected by the discrimination setup. To eliminate the loss of electronic efficiency and to achieve a value close to 100% it is necessary to find another solution to the TFC approximation problem. The effect-to-background ratio is significantly enhanced for MultiCon module and we ascribe this result to low gamma sensitivity of ND screen as well as to discrimination setup efficiency.

The comparison of resolution capability was performed for high-resolution spectra, which were registered simultaneously (see Figure 6). In this regard new MultiCon module surpasses that of DPR due to elaborated tailoring to TFS with conical surface fragments instead of plain glass scintillators used so far. Besides, the sensitive layer thickness decrease with respect to lithium glass also contributes to geometrical component reduction.

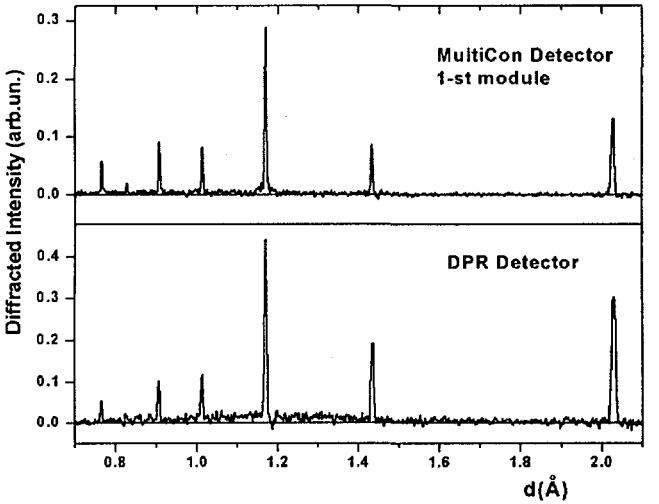

Figure 6. High-resolution diffraction patterns of α-Fe recorded simultaneously by DPR at $2\theta = 90°$ and MultiCon at $2\theta = 107.5°$ detectors at the FSD instrument and plotted against interplanar spacing d_{hkl}.

Intrinsic noise and gamma sensibility of MultiCon detector modules were measured in individual off-beam experiment. The measurements were performed for the module installed in operating position two weeks after the IBR-2 reactor shutdown and following a preliminary background study.

7. CONCLUSIONS

The results of the test carried out demonstrate several advantages of the modules based on ND screen and WLS fibers readout in comparison with detectors of previous generation. Physical properties of ZnS(Ag) scintillator enable to provide a low gamma sensitivity of the detector, and as a result to enhance its effect-to-background ratio. ND

screen flexibility and the simplicity of its processing allow to improve significantly the accuracy of TFS approximation and consequently the geometry component of a diffractometer resolution function may be reduced. Light collection with the help of WLS fibers is a cost-effective design approach drastically diminishing a number of photomultipliers, which are the most expensive elements of scintillation detectors.

Considerable drawbacks of this type detector, such as a relatively low nuclear efficiency and limited counting ability may be compensated by the usage of sandwich-like screen-fibers structures and by the division of a counter sensitive area into optically independent parts.

The first two elements of FSD detector have been manufactured and enabled to perform first physical experiments at the diffractometer in high-resolution mode. The obtained parameters of diffraction spectra (intensity, resolution, background level and d_{hkl} range) met our expectations.

ACKNOWLEGEMENTS

The authors want to thank V.L. Aksenov for support and useful discussions, and A.V. Tamonov for help in diffraction experiments. The work was financed by JINR in the frame of the JINR and BMBF (Germany) agreement on co-operation.

REFERENCES

1. V.A. Kudryashev, V.A. Trounov, V.G. Mouratov, Physica B, v. 234-236, p.1138 (1997).
2. V.L. Aksenov, A.M. Balagurov, V.G. Simkin, V.A. Trounov, P. Hiismaki et al., J. Neutron Research, v.5, p.181 (1997).
3. V.L. Aksenov, A.M. Balagurov, G.D. Bokuchava, V.V. Zhuravlev, E.S. Kuzmin, A.P. Bulkin, V.A. Kudryashev, V.A. Trounov. Communication of JINR P13-2001-30, Dubna, 2001.
4. Applied Scintillation Technologies LTD. 8 Roydonbury Industrial Estate. HARLOW CM19 5BY UK.
5. C.M. Combes, P. Dorenbos, R.W. Hollander, C.W.E. van Eijk, Nucl. Insr. and Meth. A 416 (1998).
6. J.M. Carpenter, Nucl. Instr. and Meth. v.47, p.179 (1967); A. Holas, J. Holas, E. Maliszewski, L. Sedlakova. JINR Communication E14-3759 (1968).
7. V.A. Kudryashev, H.G. Priesmeyer, J.M. Keuter, J. Schroder, R. Wagner, V.A. Trounov. Nucl. Insr. and Meth. B 93 (1994).
8. BICRON. 12345 Kingsman Road Newbury, Ohio 44065-9577, USA.
9. Photonis. Avenue Roger Roncier, Z.I. Beauregard, B.P. 520. 19106 BRIVE. FRANCE.

Received by Publishing Department
on October 1, 2001.

SUBJECT CATEGORIES OF THE JINR PUBLICATIONS

Index	Subject
1.	High energy experimental physics
2.	High energy theoretical physics
3.	Low energy experimental physics
4.	Low energy theoretical physics
5.	Mathematics
6.	Nuclear spectroscopy and radiochemistry
7.	Heavy ion physics
8.	Cryogenics
9.	Accelerators
10.	Automatization of data processing
11.	Computing mathematics and technique
12.	Chemistry
13.	Experimental techniques and methods
14.	Solid state physics. Liquids
15.	Experimental physics of nuclear reactions at low energies
16.	Health physics. Shieldings
17.	Theory of condensed matter
18.	Applied researches
19.	Biophysics

Кузьмин Е.С. и др. E13-2001-204
Детектор дифрактометра ФСД на основе сцинтилляционного экрана $ZnS(Ag)/^{6}LiF$ и сбором света с помощью спектросмещающих волокон

На реакторе ИБР-2 (ЛНФ ОИЯИ) создается специализированная установка — фурье-дифрактометр (ФСД) — для измерения внутренних напряжений в объемных изделиях и материалах методом нейтронной дифракции высокого разрешения. Одним из принципиальных узлов ФСД является детектор нового типа с комбинированной электронно-геометрической фокусировкой, сочетающий большой телесный угол регистрации с малым геометрическим вкладом в функцию разрешения. Первые два модуля детектора на базе сцинтилляционного экрана $ZnS(Ag)/^{6}LiF$ и сбором света с помощью спектросмещающих волокон были созданы и испытаны на пучке реактора ИБР-2. Описана конструкция детектора и электроника обработки сигнала. Предложен метод аппроксимации поверхности временной фокусировки, использующий гибкость экрана. Представлены характеристики испытанных модулей в сравнении с детектором предыдущего поколения и обсуждаются преимущества новой схемы детектора для дифрактометрии высокого разрешения.

Работа выполнена в Лаборатории нейтронной физики им. И.М.Франка ОИЯИ.

Препринт Объединенного института ядерных исследований. Дубна, 2001

Kuzmin E.S. et al. E13-2001-204
Detector for the FSD Fourier-Diffractometer Based on $ZnS(Ag)/^{6}LiF$ Scintillation Screen and Wavelength Shifting Fibers Readout

At the IBR-2 pulsed reactor (FLNP, JINR, Dubna), a specialized time-of-flight instrument Fourier-Stress-Diffractometer (FSD) intended for the measurement of internal steresses in bulk samples by using high-resolution neutron diffraction is under construction. One of the main components of the diffractometer is a new-type detector with combined electronic — geometrical focusing uniting a large solid angle and a small geometry contribution to the instrumental resolution. The first two modules of the detector, based on scintillation screen $ZnS(Ag)/^{6}LiF$ with wavelength shifting fibers readout have been developed and tested. The design of the detector and associated electronics are described. The method of time focusing surface approximation, using the screen flexibility is proposed. Characteristics of tested modules in comparison with a detector of previous generation are presented and advantages of new detector design for high-resolution diffractometry are discussed.

The investigation has been performed at the Frank Laboratory of Neutron Physics, JINR.

Preprint of the Joint Institute for Nuclear Research. Dubna, 2001

Макет Т.Е.Попеко

Подписано в печать 18.10.2001
Формат 60 × 90/16. Офсетная печать. Уч.-изд. л. 1,46
Тираж 325. Заказ 52911. Цена 1 р. 75 к.

Издательский отдел Объединенного института ядерных исследований
Дубна Московской области